Critique of the Wigner tunneling speed and a proposed alternative

P. Krekora, Q. Su, and R. Grobe

Intense Laser Physics Theory Unit and Department of Physics, Illinois State University, Normal, Illinois 61790-4560

In the context of superluminal propagation of wave packets through potential barriers, the tunneling speed is usually characterized by the Wigner velocity. We propose an alternative speed that takes into account the interference between the incoming and the reflected waves and leads to a better estimation of arrival time for a wave packet entering the tunneling region. This arrival time is derived by an extrapolation from inside the barrier. The analytical theory is based on the stationary phase approximation whose validity is justified by a comparison with the numerical solution of the time-dependent Dirac equation.

I. INTRODUCTION

The phenomenon of tunneling, in which a particle approaches a repulsive barrier with a height that exceeds the total energy of the particle, is usually used as an example to illustrate the different predictions from classical and quantum theory. In fact, classical mechanics predicts zero transmission while quantum mechanics predicts a nonzero transmission and is in agreement with experiments. This effect is extremely important and has been studied widely.

One exciting aspect of the tunneling process is the prospect of superluminal transmission already recognized in the original study of Wigner in the 1950s [1]. There has been a large body of theoretical work since then, addressing the issue of superluminality and causality [2–7]. Steinberg, Kwiat, and Chiao have addressed the realization of superluminal speeds [3,5]. They used a periodic potential barrier to demonstrate experimentally that superluminal velocities can indeed be obtained, and showed that this result does not violate causality.

The dynamics of quantum-mechanical electron wave tunneling can be mapped to the electrodynamics of evanescent waves. It has been studied recently, both theoretically and experimentally. Experimental data have been obtained for the tunneling of optical pulses in photonic band gaps [8], in frustrated total internal reflection [9,10], and in dielectric media [11,12]. Other potential applications of superluminal pulse propagation include instantons in particle physics, and the Josephson effect in semiconductor materials [13].

Many of the theoretical studies about superluminal wave propagation are based on the method of stationary phase approximation. The wave packets, for which this approximation does not apply, have not been investigated. In addition, several all theoretical works relied on the framework of nonrelativistic quantum theory based on the Schrödinger equation. It is obvious that such a theory has a potential deficiency in accurately addressing the question of causality. For the special case of nonrelativistic tunneling, the question of how much time it takes a particle to pass the barrier, has triggered considerable controversial debates to the present day.

It is somewhat surprising that most tunneling velocities defined thus far have to be based on averages over the entire barrier region. The microscopic dynamics under the barrier has not been investigated directly. By the early 1990s the physics community has largely accepted the existence of a time associated with the duration of tunneling, but there is still a lack of consensus with regard to the unique expression for this time scale and on the exact implications of this expression [16]. Hauge and Stovneng [14] stated that, with the exception of two candidates, all expressions for tunneling times have logical flaws, sufficiently serious that they must be rejected. The only survivors are the dwell time [15] and the asymptotic phase time [6,14], which have complementary weaknesses.

In view of the above weakness, we have recently developed a method [16,17], which allowed us to address the superluminal problem beyond the stationary phase approximation. Our quantum theory was fully relativistic, permitting us to study the violation of causality. We demonstrated that superluminality does occur in the theory based on the space-time resolved solution of the Dirac equation. In fact, we showed that particles travel with a higher speed in the Dirac theory than in the Schrödinger theory. Qualitatively the two theories were similar but the quantitative predictions were substantially different.

We have defined, for the first time, an instantaneous tunneling velocity that can be calculated for regions both inside and outside of the barrier [16]. The new velocity led to a more microscopic understanding of the transmission of the wave packet across the tunneling region. We found that superluminal velocities may imply the violation of causality only in the framework of the Schrödinger equation. Causality is not violated in the Dirac theory.

Two important issues that have not been addressed in the previous investigation [16] are the focus of the present paper. We consider first the effect due to the reflected wave packet, which has been neglected up to now. We focus in particular on how the reflected wave interferes with the incoming wave. We would like to determine how the interference changes and complicates the evaluation of the arrival time. In this paper we propose to compute the arrival time by extrapolating the instantaneous velocity from the barrier region to near the entrance interface. The instantaneous velocity in the barrier region turns out to be a smooth function of location, which makes the extrapolation straightforward and free of ambiguity. We find the computed arrival time can differ significantly from what was reported in Wigner's origi-

nal paper. We also study the significance of relativity due to multiple spinor components versus a single component.

The paper is organized as follows. The model and theoretical method are introduced in Sec. II. Details of the tunneling dynamics obtained from numerical simulations are presented in Sec. III. The new arrival time has been calculated in the stationary phase approximation in Sec. IV by extrapolating the instantaneous tunneling speed from the barrier region. We then compare this tunneling velocity with the Wigner tunneling speed across the barrier in Sec. V for various relativistic conditions. The paper ends with a summary and a brief discussion.

II. RELATIVISTIC TUNNELING DYNAMICS

We begin our analysis with an overview of the wave-packet motion. In our calculations an electron is represented by a relativistic wave packet described by the space-time dependent Dirac spinor wave function $\Psi(x,t)$ $=(\Psi_1,\Psi_2,\Psi_3,\Psi_4)$. This wave function is defined on a numerical space-time grid. In all of our simulations the spatial axis was typically discretized into at least 65 536 grid points, which, together with up to 1 500 000 temporal points, led to fully converged results [17].

The incoming electron wave packet is assumed to take the Gaussian form

$$\Psi(x,t=0)=N\exp[-(x-x_0)^2/(4\Delta x^2)]\exp(ikx)\psi(k),$$
$$(2.1)$$

where the spinor $\psi(k)$ is given by $(1,0,ck/(E+2c^2),0)$ and the normalization factor $N\equiv\{(E+2c^2)/[2(E+c^2)\Delta x\sqrt{2\pi}]\}^{1/2}$ in atomic units. Here the total energy E is $\sqrt{[c^4+c^2k^2]}-c^2$. The central canonical momentum k is related to the initial speed v via the expression $v=k/\sqrt{[c^2+k^2]}$.

The evolution of the four spinors follows the time-dependent Dirac equation in one spatial dimension:

$$i\partial\Psi/\partial t=-ic\alpha_x\partial\Psi/\partial x+c^2\beta\Psi+W(x)\Psi. \quad (2.2)$$

Here, α_x and β denote the usual Dirac matrices. The repulsive potential $W(x)$ is centered around $x=0$ and has an effective width of w and a height W. We have used a variety of tunneling potentials characterized by $W(x)=W\exp[-(2x/w)^n]$. For large (even) integers n, we recover the rectangular barrier for which the energy eigenstates can be found analytically and some approximate analytical estimates can be made. The Dirac equation (2.2) has been solved numerically using a split-operator algorithm based on fast-Fourier transformation that is accurate up to fifth order in time [17].

The initial location of the wave packet x_0 was chosen far enough to the left of the barrier so that it does not overlap with the space to the right of the barrier at time $t=0$. The potential height W was chosen to be 1.5 times the kinetic energy E such that we can practically exclude the effect of high-momentum contributions that can simply pass over the barrier without tunneling. The potential height W was chosen smaller than $2c^2$ to avoid the effect of the negative energy
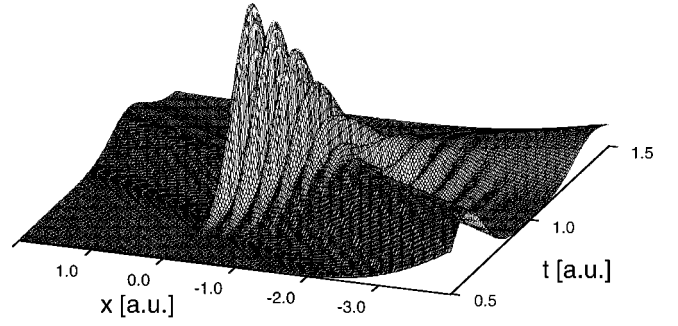

FIG. 1. The time evolution of the probability density of the relativistic wave packet during the tunneling process. (The parameters were $x_0=-10$ a.u., $\Delta x=1$ a.u., $v=10$ a.u., $w=0.1$ a.u., and $W=1.5E$.)

continuum characteristic of the so-called Klein paradox [17–19]. This restricts our initial velocities to $v<0.94c$.

In Fig. 1 we display the wave-function solution of the time dependent Dirac equation as a function of time and space. The probability density of the wave packet is given by

$$P(x,t)=\sum_{i=1}^{4}|\Psi_i(x,t)|^2, \quad (2.3)$$

where Ψ_i are the four Dirac spinor components. Figure 1 shows the injection of a wave packet (its probability density is plotted from $x<0$ toward a potential barrier at $x=0$. After a complicated interaction of tunneling in the barrier region, a reflected and a transmitted part can be clearly identified in the figure. It is worthwhile to mention that interference occurs just before the barrier where the reflected wave traveling backwards meets with the incident wave. This interference will alter the formation of the true peak in the wave packet as it ''enters'' the barrier; this will be analyzed in more detail in Sec. III.

III. THE MICROSCOPIC PICTURE
OF THE TIME-RESOLVED TUNNELING PROCESS

The sketch in Fig. 2 displays the spatial-temporal trajectory associated with the peak of the moving wave packet. The curve before approaching the barrier starts out as a straight line characteristic of a free propagation. When the wave packet approaches the barrier it begins to bend, and a time delay occurs that is caused by the reflection and the interference displayed in Fig. 1. Only a small part of a wave packet penetrates the barrier. In the direct proximity of the potential, the trajectory bends even more. Eventually it splits into two lines corresponding to the tunneled and the reflected parts of the wave packet.

The traditional Wigner tunneling speed for a wave packet tries to describe the duration of time the particle spends under the potential barrier. The precise instant in time when the wave packet leaves the right edge of the barrier at $x=w/2$, is denoted by t_B. It can be unambiguously determined by tracing the peak of the transmitted wave packet back in time to $x=w/2$. Since this emerging wave packet is usually quite
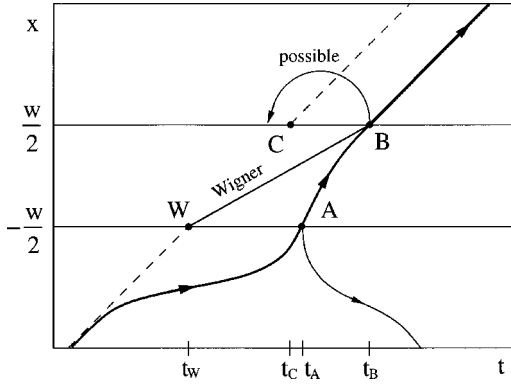
FIG. 2. The location x as a function of the temporal-peak time. The dashed line is associated with a free wave packet in the absence of any scattering potential. In this approximation, point W in the sketch indicates when a free wave packet reaches the left edge of the potential barrier and point C indicates when it departs from the tunneling region. The heavy-solid line indicates how an actual trajectory may differ from the Wigner approximation. Point A is the correct entry point to the barrier and point B is the emerging point. Points B and W are usually used to define the Wigner speed. The new tunneling speed is defined by points A and B, allowing possible interference between the reflected and the incident waves.

smooth, the determination of its peak may be carried out reliably.

More controversial and much more difficult to determine is the precise moment in time (t_A) when the electron enters the barrier. This estimation is nontrivial due to the complicated interference patterns between the incoming and reflected wave packet. In the traditional approach by Wigner, an entry time, denoted by t_W, has been associated with the time when a freely propagating wave packet would strike the edge. This time can be easily obtained by extrapolating the incoming trajectory (dashed line) to the left edge of the barrier at $x=-w/2$, as marked by point W. We should note, however, that this assumption neglects important effects due to the reflected wave. The interference may even produce a multipeak structure resulting in a significant modification of the arrival time for the incoming wave. In order to make a better estimation of the time spent in the tunneling region, one has to find a more accurate method to calculate the arrival time.

If there were no barrier present, the electron would have arrived at $x=w/2$, at the time associated with point C. De-

pending on the choice of the parameters, the point C can be either to the left or to the right of point B, associated with a Wigner tunneling speed $w/(t_B-t_W)$ larger or smaller than the velocity of the incoming wave packet.

Let us now describe an improved arrival time (denoted in the sketch by t_A), that can differ significantly from the traditional Wigner arrival time t_W. This time is based on extrapolating the center of the transmitted wave packet back in time through the barrier to the left edge $x=-w/2$. We should note that, in this approach, the interference between the incoming and the reflected wave packets is taken into account.

The wave function in the tunneling region decays approximately exponentially as a function of space. This function is obviously not localized (it does not have a local maximum) if a snapshot of the wave function is taken at any moment of time. A conventional definition of a velocity, however, relies on how a "spatial peak" of a state has moved between two snapshots. This scheme faces a challenge inside the potential barrier, where it is not possible to find a spatial peak. To resolve this problem we note that even though the wave function is not spatially localized, the probability density is *temporally localized* for each position inside of the tunneling region. In other words, as the wave packet tunnels through the barrier, there is a precisely defined time for each position at which the spatial probability takes its maximum value. At such an instance, the peak time uniquely specifies "when" the particle "passes" the selected point in space. Using this concept permits us (a) to define an improved arrival time t_A and therefore an improved average tunneling speed $w/(t_B-t_A)$, and (b) we can even define an instantaneous velocity under the barrier that matches the conventional velocity at the right end of the barrier.

Before we compare this new tunneling velocity with the traditional Wigner speed in Sec. V, let us first derive some analytical results for the relevant times using the known analytical form for the relativistic energy eigenstates for a rectangular potential.

The time t_W can be easily obtained by extrapolating the incoming wave packet in the absence of any reflection:

$$t_W = -\frac{c^2+E}{c^2 k}(w/2+x_0). \tag{3.1}$$

In the presence of the barrier, the wave packet actually emerges from the barrier at point B. Below we will derive an analytical estimate of this time:

$$t_B = \frac{\Gamma}{2\kappa^2}\frac{(1+\Gamma^{-2})\left(1+\dfrac{k^2}{\kappa^2}\right)\tanh(\kappa w)-(1-\Gamma^{-2})\kappa w\,\dfrac{c^2-(W-E)}{c^2}\,\mathrm{sech}(\kappa w)}{1+\dfrac{1}{4}(\Gamma-\Gamma^{-1})^2\tanh^2(\kappa w)}-\frac{c^2+E}{c^2 k}(w/2+x_0), \tag{3.2}$$

where

$$\kappa \equiv \frac{1}{c}\sqrt{c^4-(E+c^2-W)^2}\quad\text{and}\quad\Gamma\equiv\sqrt{\frac{E(E+2c^2-W)}{(E+2c^2)(W-E)}}.$$

The same stationary phase analysis will also lead to an expression for the correct arrival time

$$t_A = \frac{\Gamma}{2\kappa^2} \frac{(1+\Gamma^{-2})\left(1+\dfrac{\kappa^2}{k^2}\right)\tanh(\kappa w) - (1-\Gamma^{-2})\kappa w \dfrac{c^2-(W-E)}{c^2}\operatorname{sech}(\kappa w)}{1+\dfrac{1}{4}(\Gamma-\Gamma^{-1})^2 \tanh^2(\kappa w)}$$

$$- \frac{k}{\kappa^3}\frac{c^2}{c^2+E} \frac{\left(1+\dfrac{\kappa^2}{k^2}\right)\tanh(\kappa w) - \left(1-\dfrac{\kappa^2}{c^2}\right)\kappa w\, \operatorname{sech}(\kappa w)}{1+\left[2\dfrac{c^2}{E+c^2}\dfrac{w}{\kappa^2}-1\right]\tanh^2(\kappa w)} - \frac{c^2+E}{c^2 k}(w/2+x_0). \tag{3.3}$$

For our analytical derivation of Eqs. (3.2) and (3.3), we assume that the spatial as well as temporal peaks may be evaluated by their corresponding expectation values, i.e., $x_p = \langle x \rangle$ and $t_p = \langle t \rangle$. These hold as good approximations for wave packets that are nearly symmetric. The form of the initial state (2.1) corresponds to a particle that is polarized in the direction of motion and we need to use only two spinor components to describe the electron. The temporal peak value t_p is a function of the position x and can be expressed as a weighted average:

$$t_p \equiv \frac{t_1 \displaystyle\int dt|\Psi_1|^2 + t_3 \displaystyle\int dt|\Psi_3|^2}{\displaystyle\int dt|\Psi_1|^2 + \int dt|\Psi_3|^2} = \frac{t_1+rt_3}{1+r}, \tag{3.4}$$

where t_1 and t_3 are the peak times associated with the first and third spinor components. Using the stationary phase approximation, these times can be approximated by

$$t_i \equiv \frac{\partial \alpha_i(x)}{\partial E}, \quad i=1,3, \tag{3.5}$$

where α_1 and α_3 are phases of the corresponding spinor components of the stationary wave function solution under the barrier:

$$\alpha_1(x) \equiv \alpha_r - \tan^{-1}\{\Gamma \tanh[\kappa(w/2-x)]\}, \tag{3.6a}$$

$$\alpha_3(x) = \alpha_r + \tan^{-1}\left[\frac{1}{\Gamma}\tanh[\kappa(w/2-x)]\right] \tag{3.6b}$$

with

$$\alpha_r = \tan^{-1}\left[\frac{1}{2}\left(\Gamma-\frac{1}{\Gamma}\right)\tanh(\kappa w)\right] + k(w/2+x_0). \tag{3.6c}$$

The probability ratio r between both spinors, can be expressed as

$$r = \frac{\displaystyle\int dt|\Psi_3|^2}{\displaystyle\int dt|\Psi_1|^2} \approx \frac{(W-E)}{2c^2-(W-E)}\frac{\Gamma^2+\tanh^2[\kappa(w/2-x)]}{1+\Gamma^2\tanh^2[\kappa(w/2-x)]}. \tag{3.7}$$

Using formula (3.5) we can evaluate the times associated with each spinor component:

$$t_1 = t_r - \frac{\Gamma}{\kappa^2}\frac{\left(1+\dfrac{\kappa^2}{k^2}\right)\tanh[\kappa(w/2-x)] - \kappa(w/2-x)\dfrac{c^2-(W-E)}{c^2}\operatorname{sech}[\kappa(w/2-x)]}{1+\Gamma^2\tanh^2[\kappa(w/2-x)]} \tag{3.8a}$$

and

$$t_3 = t_r - \frac{\Gamma}{\kappa^2}\frac{\left(1+\dfrac{\kappa^2}{k^2}\right)\tanh[\kappa(w/2-x)] + \kappa(w/2-x)\dfrac{c^2-(W-E)}{c^2}\operatorname{sech}[\kappa(w/2-x)]}{\Gamma^2+\tanh^2[\kappa(w/2-x)]} \tag{3.8b}$$

with the parameter t_r given by

$$t_r = \frac{\Gamma}{2\kappa^2}\frac{(1+\Gamma^{-2})\left(1+\dfrac{\kappa^2}{k^2}\right)\tanh(\kappa w) - (1-\Gamma^{-2})\kappa w \dfrac{c^2-(W-E)}{c^2}\operatorname{sech}(\kappa w)}{1+\dfrac{1}{4}(\Gamma-\Gamma^{-1})^2\tanh^2(\kappa w)} - \frac{c^2+E}{c^2 k}(w/2+x_0). \tag{3.8c}$$
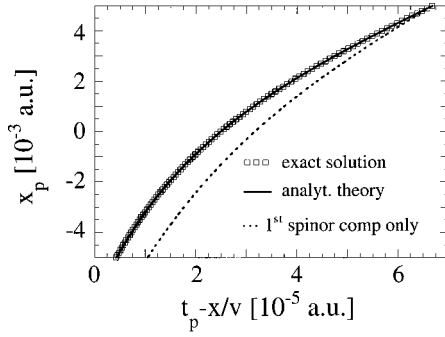
FIG. 3. The peak position x_p as a function of the (shifted) temporal-peak time. The open squares are the exact numerical solutions and the solid line denotes the prediction according to the analytical formula [Eq. (3.4)] based on the stationary phase approximation. The dashed line is calculated from considering only the first spinor component of the wave function. (The parameters were $x_0 = -100$ a.u., $\Delta x = 20$ a.u., $v = 100$ a.u., $w = 0.01$ a.u., and $W = 1.5E$.)

Combining these expressions, we obtain $t_p(x)$ and the departure and arrival times become: $t_B = t_p(x = w/2)$ and $t_A = t_p(x = -w/2)$ as presented in Eqs. (3.2) and (3.3).

To perform the stationary phase analysis we had to meet the requirement that the probability $P(x,t)$ is well localized in the momentum space around a single maximum around k. Fortunately, this is fulfilled for most practical cases.

In order to establish the validity of this analytical estimate, we show in Fig. 3 the quantum trajectory under the barrier calculated from the exact numerical wave function solution to the Dirac equation. At each position under the barrier, we have computed that time at which the wave function takes its largest value. In our calculations, we have chosen the barrier to extend from -5×10^{-3} to 5×10^{-3} a.u. The wave packet is prepared at time $t_0 = 0$ at $x_0 = -100$ a.u. and it moves towards the positive part of the space with an initial velocity of $v = 100$ a.u. This exact curve is superimposed with the analytical formula $t_p = t_p(x)$ given by Eq. (3.4). The two curves are practically indistinguishable. This justifies nicely our two key assumptions (a) to associate the maximum time t_p with its average $\langle t \rangle$ to evaluate the contributions of each spinor, and (b) to use the stationary phase approximation. The third curve (the dashed line) corresponds to a quantum trajectory; however, it is calculated only from the first spinor component of the wave packet. The difference between the curves illustrates the importance of the third spinor component under the barrier. A similar comparison for the transmitted wave packet suggests that, in contrast to the state under the barrier, the third component is less important outside the barrier.

In our method, the peak time is a function of the position x, even though in Fig. 3, space is arranged vertically and time horizontally. Such an arrangement leads to a slope that must be interpreted as an instantaneous velocity. In the following sections we will discuss the properties of this instantaneous velocity and compare its average value to the traditional Wigner speed.

IV. THE INSTANTANEOUS TUNNELING VELOCITY

In this section we analyze the instantaneous (position dependent) velocity defined as the slope of the curve presented in Fig. 3:

$$v_T(x) \equiv \left[\frac{dt_p}{dx} \right]^{-1}. \tag{4.1}$$

Considering the first and third spinor components, it can be rewritten as

$$v_T = \frac{1+r}{t_1' + r t_3' - r'(t_p - t_3)}, \tag{4.2}$$

where the primes denote the spatial derivatives, and

$$r' = \frac{dr}{dx} = \kappa \frac{(\Gamma^4 - 1)\sinh[2\kappa(w/2 - x)]}{\{\Gamma^2 \cosh^2[\kappa(w/2 - x)] + \sinh^2[\kappa(w/2 - x)]\}^2}. \tag{4.3}$$

Instead of presenting the lengthy expression for the instantaneous velocity, let us examine the (simpler) expressions for regions close to either edge of the barrier.

As shown in Fig. 3, the instantaneous velocity v_T is largest at $x = -w/2$ and then decreases with the barrier penetration depth. The instantaneous velocity close to the barrier's right edge [for $\kappa(x - w/2) \ll 1$] can be simplified to

$$v_T \approx \left[1 + 4 \frac{c^2(\Gamma^2 + 1)}{2c^2 - (W - E)(\Gamma^2 - 1)} [\kappa(w/2 - x)^2] \right] v_{\text{free}}. \tag{4.4}$$

Here v_{free} is the velocity of the outgoing (transmitted) wave packet in free space, which is typically close to the incoming speed v.

It is worth noting that Eq. (4.4) predicts that the velocity is only a function of $x - w/2$ near the edge. In other words, the instantaneous velocity in the proximity of the right edge does not depend on the width of the barrier. This remarkable fact is illustrated in Fig. 4. We compare the position dependent speed for two barriers with length $w = 0.01$ and $w = 0.005$ a.u. Both barriers have their right edge at $x = 0.005$ a.u. The perfect coincidence of the lines for the different barrier widths seen here, extends almost through the entire region of the shorter barrier and suggests that one may expect the same universal behavior of the tunneled wave packet, regardless of the total width of the barrier. As long as the incident energy of the packet and the height of the potential remain the same, the only important parameter is the distance of the peak to the right edge of the barrier.

In contrast, the instantaneous velocity at the left edge of the barrier depends strongly on the barrier width. On the other hand, for barriers [$1 \ll \kappa(x - w/2)$] it can be approximated by

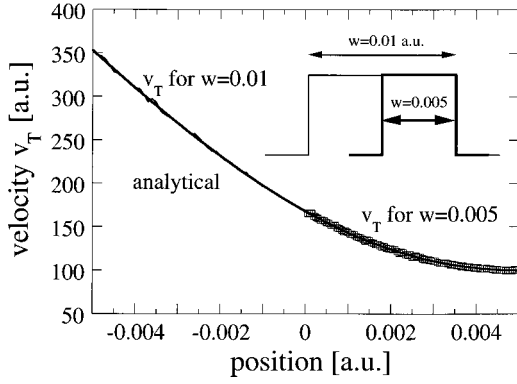$$v_T \approx \frac{\kappa}{\Gamma} \frac{1 + \Gamma^2}{1 + (\kappa/k)^2} \cosh^2[\kappa(w/2 - x)], \tag{4.5}$$

FIG. 4. The instantaneous velocity as a function of the position. The thick-solid line is the analytical solution [Eq. (4.2)]. The thin line corresponds to numerical simulation. The squares are the numerical predictions for a barrier of width $w = 0.005$ a.u. The inset illustrates the configuration of the two potentials. (The parameters were $x_0 = -100$ a.u., $\Delta x = 20$ a.u., $v = 100$ a.u., $w = 0.01$ a.u., and $w = 0.005$ a.u., and $W = 1.5E$.)

which diverges strongly with the barrier width w. This behavior can be linked to the Hartmann effect [20], as we will discuss in Sec. V.

V. COMPARISON OF THE WIGNER VELOCITY WITH THE (AVERAGED) INSTANTANEOUS VELOCITY

Let us now compare the Wigner $\bar{v}_w = w/(t_B - t_w)$ and the average tunneling velocity $\bar{v}_T = w/(t_B - t_A)$. This velocity is a *time* average of the instantaneous velocity: $\bar{v}_T = 1/(t_B - t_A)\int_{t_A}^{t_B} dt\, v_T[x(t)]$. On the other hand, the spatially averaged velocity $(1/w)\int_{-w/2}^{w/2} dx\, v_T[x]$ is different than $\bar{v}_T$ because the trajectory $x_p(t)$ is a nonlinear function of time.

It can be shown that when the tunneled wave packet is not distorted significantly, the speed can be rewritten as

$$\bar{v}_T = \frac{(1+a)w}{\partial(\Delta\alpha_1)/\partial E + a\,\partial(\Delta\alpha_3)/\partial E}, \qquad (5.1a)$$

where

$$a \equiv \frac{\Gamma^4(1+\tanh^2\kappa w)+2\Gamma^2}{2(1+\Gamma^2\tanh^2\kappa w)} \qquad (5.1b)$$

and $\Delta\alpha_{1,3}$ is the phase difference between right and left edges for the first and the third component, respectively:

$$\Delta\alpha_1 = \tan^{-1}[\Gamma\tanh(\kappa w)], \qquad (5.1c)$$

$$\Delta\alpha_3 = \tan^{-1}\left[\frac{1}{\Gamma}\tanh(\kappa w)\right]. \qquad (5.1d)$$

Similarly we may rewrite the Wigner velocity as

$$\bar{v}_w = \frac{w}{\partial(\Delta\alpha_w)/\partial E}. \qquad (5.2)$$

Here $\Delta\alpha_w$ is the phase difference (which is identical for the first and the third components) between outgoing and incoming waves without considering interference:

$$\Delta\alpha_w = \tan^{-1}\left[\frac{1}{2}\left(\Gamma - \frac{1}{\Gamma}\right)\tanh(\kappa w)\right]. \qquad (5.3)$$

The expressions (5.1) may be written explicitly as

$$\bar{v}_T = \kappa w\frac{\kappa^2}{k}\left(1+\frac{E}{c^2}\right)$$
$$\times \frac{1+\left[2\frac{c^2}{E+c^2}\frac{V}{\kappa^2}-1\right]\tanh^2(\kappa w)}{\left(1+\frac{\kappa^2}{k^2}\right)\tanh(\kappa w)-\kappa w\left(1-\frac{\kappa^2}{c^2}\right)\text{sech}(\kappa w)}$$

$$(5.4a)$$

and the relativistic Wigner speed is

$$\bar{v}_w = \frac{w\kappa^2}{2\Gamma}\frac{4\Gamma^2+(\Gamma^2-1)^2\tanh^2(\kappa w)}{(\Gamma^2+1)\left(1+\frac{\kappa^2}{k^2}\right)\tanh(\kappa w)-(\Gamma^2-1)\kappa w\frac{c^2+E-W}{c^2}\text{sech}(\kappa w)}. \qquad (5.4b)$$

The main difference between the Wigner and averaged instantaneous velocity arises from a delay on the incident edge of the barrier. Figure 5 presents a comparison between these two velocities as a function of the barrier width w. Because this delay is related to the interference between the incident and reflected components, the temporal peak at the incident edge is formed later than the one of the freely propagating packet. This delay makes the averaged instantaneous velocity always larger than the Wigner velocity. Another important difference is that the tunneling speed $\bar{v}_T$ is always

larger than the incident velocity v. In the limit of a very thin barrier, the tunneling speed $\bar{v}_T$ becomes identical to the incident velocity

$$\lim_{w\to 0}\bar{v}_T = v. \qquad (5.5a)$$

This agreement makes $\bar{v}_T$ a much more physically reasonable speed compared to $\bar{v}_W$. The Wigner velocity is less "physical" as $\bar{v}_W$ can be even smaller than the incident ve-
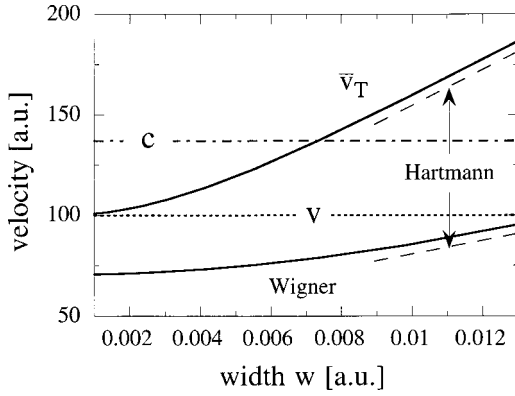
FIG. 5. Average tunneling velocities: Wigner velocity (lower line) and average tunneling velocity $\bar{v}_T$ (upper line) as a function of the barrier width. Both curves asymptotically approach straight lines for large width w. (The parameters were $x_0 = -100$, $\Delta x = 20$, $v = 100$ a.u., and $W = 1.5E$.)

locity for very thin barriers, as the fast tunneling process does not have enough "space" to make up for the delay at the left edge:

$$\lim_{w \to 0} \bar{v}_w = \frac{\Gamma \kappa}{[1 + (\kappa/k)^2 + (E - w)/c^2]} v. \qquad (5.5b)$$

It is quite remarkable that in the opposite limit of a wide barrier $(1 \ll \kappa w)$, both velocities increase linearly with the width, however, with significantly different slopes, which are off by a factor of 2:

$$\lim_{w \to \infty} \bar{v}_T = \frac{(1 + \Gamma^2)k^2 \kappa^2}{\Gamma(k^2 + \kappa^2)} w, \qquad (5.6a)$$

$$\lim_{w \to \infty} \bar{v}_w = \frac{(1 + \Gamma^2)k^2 \kappa^2}{2\Gamma(k^2 + \kappa^2)} w. \qquad (5.6b)$$

The linear dependence of velocity on the barrier width is well-known from nonrelativistic tunneling such as the Hartmann effect. It leads to a finite limit for the tunneling time. This implies that the delay from the Wigner arrival time is the same as the time it takes for the wave packet to travel across the barrier.

VI. DISCUSSION

In the present paper we discussed the properties of the recently introduced instantaneous velocity [16], as well as its

connection with the Wigner tunneling speed. We have corrected the arrival time for a wave packet entering the tunneling barrier. This correction has considered the interference between the reflected and the incoming waves neglected in the Wigner theory. We showed that the spatial characteristics of the instantaneous velocity are very similar for barriers with the same right edge and height regardless of the barrier width. This universality of the speed is quite interesting from the point of view of causality. Usually, the velocity of a particle at a given position depends, in classical mechanics, on its past trajectory and one could (incorrectly) conjecture that the tunneling velocity under the barrier should therefore be a function of the distance to the left edge. However, it turns out that the instantaneous tunneling speed depends on the distance to the right edge, and not on the location of the left edge. Due to its conserved energy, the particle is confined to leave the right edge with a velocity close to the incoming velocity. The main dynamics of the tunneling, however, is determined at the left edge by the significant interferences between incoming and reflected wave packets. The details of this interference, however, depend on the total width of the potential and therefore the location of the right edge.

Most of our analysis was based on the stationary phase approximation, which is reliable for wave packets that are nearly symmetric. The analytical formulas were evaluated at proper values of the momentum k. This was possible because the state depends only very weakly on the momentum as the spatial wave-packet spreading was not so important [21,22]. On the other hand, for wave packets that are prepared relatively far from the barrier, different momenta components can become spatially separated from each other before they reach the barrier location. As a consequence it may happen that the tunneled peak can leave the barrier even before the incident one hits the barrier. We have also illustrated that in the relativistic regime, it is important to consider different spinor components in computing the arrival time for comparison with a possible experiment.

[1] E. P. Wigner, Phys. Rev. **98**, 145 (1955).

[2] C. R. Leavens and G. C. Aers, Phys. Rev. B **40**, 5387 (1989).

[3] R. Y. Chiao, P. G. Kwiat, and A. M. Steinberg, Physica B **175**, 257 (1991).

[4] T. Martin and R. Landauer, Phys. Rev. A **45**, 2611 (1992).

[5] A. M. Steinberg, P. G. Kwiat, and R. Y. Chiao, Phys. Rev. Lett. **73**, 2308 (1994).

[6] R. Landauer and T. Martin, Rev. Mod. Phys. **66**, 217 (1994).

[7] V. Gasparian, M. Ortuno, J. Ruiz, and E. Cuevas, Phys. Rev. Lett. **75**, 2312 (1995).

[8] C. Spielmann, R. Szipöcs, A. Stingl, and F. Krausz, Phys. Rev. Lett. **73**, 2308 (1994).

[9] A. M. Steinberg, P. G. Kwiat, and R. Y. Chiao, Phys. Rev. Lett. **71**, 708 (1993).

[10] V. Gasparian, M. Ortuno, J. Ruiz, and E. Cuevas, Phys. Rev. Lett. **75**, 2312 (1995).

[11] Ph. Balcou and L. Dutriaux, Phys. Rev. Lett. **78**, 851 (1997).

[12] L. J. Wang, A. Kuzmich, and A. Dogariu, Nature (London) **406**, 277 (2000).

[13] For a review, see, e.g., F. Capasso, K. Mohammed, and A. Y. Cho, Int. J. Quantum. Electron. **QE-22**, 1853 (1986).

[14] E. H. Hauge and J. A. Stovneng, Rev. Mod. Phys. **61**, 917 (1989).

[15] F. T. Smith, Phys. Rev. **118**, 349 (1960); M. Büttiker, in *Electronic Properties of Multilayers and Low Dimensional Semiconductors*, edited by J. M. Chamberlain, L. Eaves, and J. C. Portal (Plenum, New York, 1990), p. 297; M. Büttiker and H.

Thomas, Ann. Phys. (Leipzig) **7**, 602 (1998).

[16] P. Krekora, Q. Su, and R. Grobe, Phys. Rev. A **63**, 032107 (2001).

[17] J. W. Braun, Q. Su, and R. Grobe, Phys. Rev. A **59**, 604 (1999).

[18] O. Klein, Z. Phys. **41**, 407 (1927); **53**, 157 (1929).

[19] W. Greiner, B. Müller, and J. Rafelski, *Quantum Electrodynamics of Strong Fields* (Springer-Verlag, Berlin, 1985).

[20] T. E. Hartman, J. Appl. Phys. **33**, 3427 (1962).

[21] Q. Su, B. A. Smetanko, and R. Grobe, Opt. Express **2**, 277 (1998).

[22] Q. Su, B. A. Smetanko, and R. Grobe, Laser Phys. **8**, 93 (1998).